Available online at www.sciencedirect.com

SciVerse ScienceDirect

Ceramics International 38 (2012) 6685–6691

CERAMICS INTERNATIONAL

www.elsevier.com/locate/ceramint

Synthesis of α-Al_2O_3 at mild temperatures by controlling aluminum precursor, pH, and ethylenediamine chelating additive

Jun Sung Lee[a], Hyun Soo Kim[a], Jun Su Lee[a], No-Kuk Park[b], Tae Jin Lee[b], Misook Kang[a,*]

[a]*Department of Chemistry, College of Science, Yeungnam University, Gyeongsan, Gyeongbuk 712-749, Republic of Korea*
[b]*School of Chemical Engineering, Yeungnam University, Gyeongsan, Gyeongbuk 712-749, Republic of Korea*

Received 18 April 2012; received in revised form 18 May 2012; accepted 18 May 2012
Available online 26 May 2012

Abstract

This study demonstrates the synthesis of α-Al_2O_3 by sol–gel method according to various reaction parameters. Various Al_2O_3 phases were synthesized by a simple sol–gel method using three different aluminum precursors (aluminum isoporoxide (AIP), $Al(OH)_3$, and AlO(OH)) and pHs (3, 7, and 9). Thermally treating of the synthesized powders at 1200 °C produced rhombohedral structure α-Al_2O_3. When AIP was used as an aluminum precursor, α-Al_2O_3 was synthesized at all pH levels by calcination at 1200 °C. The structure was easily changed to α-Al_2O_3 by the addition of ethylenediamine as a chelating additive at the lower temperature of 1000 °C. In contrast, no α-Al_2O_3 structure was obtained by using $Al(OH)_3$ or AlO(OH) precursors at higher pH in spite of thermal treatment at 1200 °C. The specific surface areas were larger in α-Al_2O_3 synthesized using AIP precursor compared with that using $Al(OH)_3$ and AlO(OH) precursors. Electrophoretic light scattering (ELS) measurement in aqueous solution at pH = 7 revealed positive surface charges in the α-Al_2O_3 synthesized using AIP precursor, but negative charges in that synthesized using $Al(OH)_3$ and AlO(OH) precursors. Most significantly, the α-Al_2O_3 synthesized with the ethylenediamine chelating additive had a negative charge, despite the use of AIP precursor, with a higher mobility and larger aggregated particle diameter.

Keywords: α-Al_2O_3; Mild temperature; Ethylenediamine chelating; Aluminum precursor

1. Introduction

Alumina is an advanced ceramic with wide applications in electrical insulating [1,2], microelectronics [3], polishing [4,5], and various material matrixes, depending on the structural diversity. Particularly, the α-Al_2O_3 powder has considerable potential for a wide range of applications including high strength materials, sapphire crystal growth [6,7], electronics, semiconductors [8] and catalysts [9,10]. Due to its versatility, increasing interest has focused on the synthesis of α-Al_2O_3. In general, α-Al_2O_3 derived from the decomposition of gelatinous boehmite [11], gibbsite [12], and related hydroxide alumina [13] undergoes a number of transitional phases. Amorphous alumina dehydrates at 500 °C to form γ-alumina which then transforms to δ-alumina and θ-alumina before becoming α-Al_2O_3 in the range of 1200–1400 °C, depending on the procedure [14,15]. However, little research is presently being conducted on the synthesis of α-Al_2O_3 because the high formation temperature makes it more difficult to create a structure at a lower temperature. In contrast, the preparation of ceramic powders through wet chemical methods, including sol–gel, has attracted considerable attention. Several studies on the preparation of α-Al_2O_3 have tried to lower the formation temperature by using additives [16,17]. It has been suggested that the metal–organic derived alumina could lower the transformation temperature of α-Al_2O_3. Such studies are continuing, but without evident success as yet. Therefore, a basic approach is needed.

In this study, we synthesize a special α-Al_2O_3 powder as a raw material for sapphire crystal growth in application to the LED industry in order to give higher crystallinity, stronger density, and greater purity. The morphologies of the α-Al_2O_3 are controlled in the preparation steps. The effects of the aluminum precursor, pH, ethylenediamine chelating additive, and thermal treatment temperature are

*Corresponding author. Tel.: +82 53 810 2363.
E-mail address: mskang@ynu.ac.kr (M. Kang).

0272-8842/$36.00
http://dx.doi.org/10.1016/j.ceramint.2012.05.057

determined in the standard sol–gel method. The as-synthesized α-Al_2O_3 powders are characterized by X-ray diffraction (XRD) analysis, transmission electron microscope (TEM), field emission scanning electron microscope (FESEM), Fourier transform infrared spectroscopy (FT-IR), specific surface area (Brunauer–Emmett–Teller, BET), X-ray photoelectron spectroscopy (XPS) measurement, and zeta potentials using electrophoresis light scattering (ELS) measurement.

2. Experimental

2.1. Synthesis of α-Al_2O_3 according to three types Al precursor, pH, and ethylenediamine chelating additive

Aluminum isoporoxide (AIP; Wako Pure Chem. Ltd.), gibbsite ($Al(OH)_3$; Wako Pure Chem. Ltd.) and boehmite (AlO(OH); Wako Pure Chem. Ltd.) were used as aluminum precursors. Acetic acid, ammonia water and ethylenediamine were used for pH control. First, the aluminum precursors of 0.1 mol and ethanol solvent of 1.0 L were well mixed until an evenly white solution was obtained for 2 h. Acetic acid, ammonia water, and ethylenediamine as a chelating additive were added to the mixed solution for pH control. The pH was fixed at 3, 7, and 9, and the final solutions were stirred homogeneously for 5 h. White powders were obtained after vacuum drying process. The powders were heated in flowing air at a rate of 10 °C/min in the range of 400–1200 °C at intervals of 200 °C, and then maintained isothermally at this temperature for at least 3 h.

2.2. Characterizations of the synthesized α-Al_2O_3

The prepared materials were identified using powder XRD (model MPD from PANalytical) with nickel-filtered CuKα radiation (30 kV, 30 mA) at 2-theta angles of 10°–80°. The scan speed was 10°/min, and the time constant was 1 s.

The sizes and shapes of the materials were measured by field emission SEM/energy-dispersive X-ray spectroscopy (FESEM/EDS; S-4100, Hitachi, Yeungnam University Instrumental Analysis Center, Korea).

XPS measurements of the Al_{2p} and O_{1s} orbitals were recorded with a model AXIS-NOVA (Kratos Inc., Korea Basic Science Institute Jeonju Center, Korea) system, equipped with a non-monochromatic AlKα (1486.6 eV) X-ray source.

The specific surface area was calculated according to the BET theory that gives the isotherm equation for multilayer adsorption by generalization of Langmuir's treatment of the unimolecular layer. The BET surface areas were measured using a Micrometrics ASAP 2000 instrument. The materials were degassed under vacuum at 120 °C for 1 h before the BET surface measurements. Then the samples were thermally treated at 300 °C for 30 min. The BET surface areas of the materials were measured through nitrogen gas adsorption using a continuous flow method with a mixture of nitrogen and helium as the carrier gas.

The zeta potentials of the materials were determined by electrophoretic mobility using an electrophoresis measurement apparatus (ELS 8000, Otsuka Electronics, Japan) with a plate sample cell. ELS determinations were performed in the reference beam mode at a laser light source wavelength of 670 nm, modular frequency of 250 Hz and scattering angle of 15°. The standard error of the zeta potentials, converted from the experimentally determined electrophoretic mobility, was typically $< 1.5\%$ and the percent error $< 5\%$. To measure the zeta potentials, 0.1 wt% of each sample was dispersed in de-ionized water and the pH of the solution was adjusted to 7. Relative molecular diameter size distributions of the various solutions were also measured by using this equipment. The zeta potential distributions were obtained by averaging 2 or 3 runs.

The FT-IR spectra were recorded on a Mattson 1000 spectrometer, using the diffused reflectance method. The powdered sample, mixed with CaF_2, was pressed into a pellet form. To reduce the influence of humidity, the pellet was kept at a temperature of 200 °C in a drying oven for 2 h prior to measurement. The scan range for the measurement ranged from 400 to 2000 cm^{-1}, with 50 scans accumulated to obtain a resolution of 4.0 cm^{-1}.

3. Results and discussion

Fig. 1 shows the XRD patterns of the α-Al_2O_3 particles thermally treated at 1200 °C and prepared at various pHs and from various aluminum precursors. The synthesized α-Al_2O_3 particles in most samples exhibited peaks at 2 theta angles of 25.57, 35.14, 37.76, 43.33, 46.16, 52.53, 57.47, 61.27, 66.49, 68.18, and 76.84, corresponding to the (d_{012}), (d_{104}), (d_{110}), (d_{113}), (d_{202}), (d_{024}), (d_{116}), (d_{018}), (d_{214}), (d_{300}) and ($d_{1,0,10}$) spaces, respectively [18]. They were ascribed to the rhombohedral structure, JCPDS file no. 88-0826. All samples from the AIP precursor exhibited a clear rhombohedral structure, regardless of the pH. Otherwise, the α-Al_2O_3 phase presented at pH = 3 and pH = 7 when using the gibbsite, $Al(OH)_3$, and only at pH = 7 when using the boehmite precursor, AlO(OH). With gibbsite at pH = 9, κ-Al_2O_3 [19] was produced and with boehmite at pH = 3 and pH = 9, θ-Al_2O_3 [20] was. These results revealed the significant effect of the initial pH on the crystallinity, because sol–gel processing is based on several chemical processes, such as hydrolysis and poly-condensation. This indicates that at low pH with AIP, the rate of hydrolysis is governed by the hydronium ion in acidic solutions, so that the amount of water is small due to rapid formation of H_3O^+. On the other hand, the reaction is controlled by the hydroxyl ions (OH^-) when powders are derived at pH = 7. The initial growth leads to a linear chain, but the high concentration of OH^- ions leads to crystallization because the probability of intermolecular reaction is higher than the intra-molecular reaction. The most probable metal–oxygen polymeric network is formed at high pH. Nonetheless, the larger interstices at pH = 9 may lead to larger grains.

Conversely the line widths of the peaks were broad, which generally indicates a smaller crystalline domain size. The full width at half maximum (FWHM) height of the peak at 2 theta = 35.14° (104) was measured, and the Scherrer equation, $t = 0.9\lambda/\beta \cos\theta$, where λ is the wavelength of the incident X-rays, β is the FWHM in radians and θ is the diffraction angle, which was used to determine the crystalline domain size. The calculated crystalline domain sizes based on a special peak of 35.14° (d_{104}) were 39.66, 39.67, 39.67, 48.07, 48.06, and 48.06 nm for the α-Al_2O_3 powders, referred to as (a)–e) and (h), respectively. This result confirmed the use of AIP as the precursor for aluminum and the importance of the pH parameter.

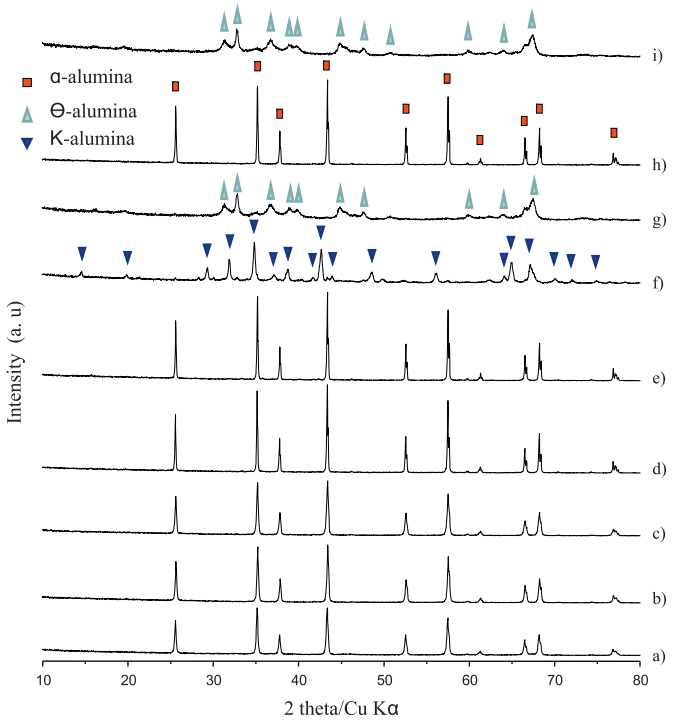

Fig. 1. The XRD patterns of the α-Al_2O_3 powders thermally treated at 1200 °C, and prepared at various pHs and aluminum precursors. (a), (b), and (c) samples synthesized with AIP precursor at pH = 3, 7, and 9, respectively; (d), (e), and (f) samples synthesized with $Al(OH)_3$ precursor at pH = 3, 7, and 9, respectively; (g), (h), and (i) samples synthesized with AlO(OH) precursor at pH = 3, 7, and 9, respectively.

Fig. 2 compares the XRD patterns of the alumina phases prepared from AIP precursor with and without ethylenediamine at various calcinations temperatures and at pH = 9. Al_2O_3 has a structurally complex oxide comprised of several different meta-stable phases, which eventually convert to stable α-Al_2O_3. When AIP precursor and the ethylenediamine (fixed at pH = 9) chelating additive were introduced, the XRD peaks that were assigned to α-Al_2O_3 were clearer and sharper in spite of the heat treatment temperature of only 1000 °C. However, no α-Al_2O_3 was produced at this temperature without ethylenediamine. Another paper [21] has reported the appearance of boehmite, γ-alumina, θ-alumina, and a mixture of θ- and γ-Al_2O_3 at 300, 500, 700, and 900 °C, respectively; however, the phases were seen at the lower temperatures when using ethylenediamine additive. Consequently, α-Al_2O_3 was easily acquired with the addition of ethylenediamine, and it lowered the existing temperature by 200 °C, compared to the previously reported result [21]. The calculated crystalline domain sizes were 39.67 and 36.04 nm at a special peak of 35.14° (d_{104}) for the α-Al_2O_3 powders, referred to as A-e and B-e, respectively. This result is proof of the effect of the organic additive in determining the growth.

FESEM–TEM images of the α-Al_2O_3 particles prepared at various pHs and Al precursors are shown in Fig. 3.

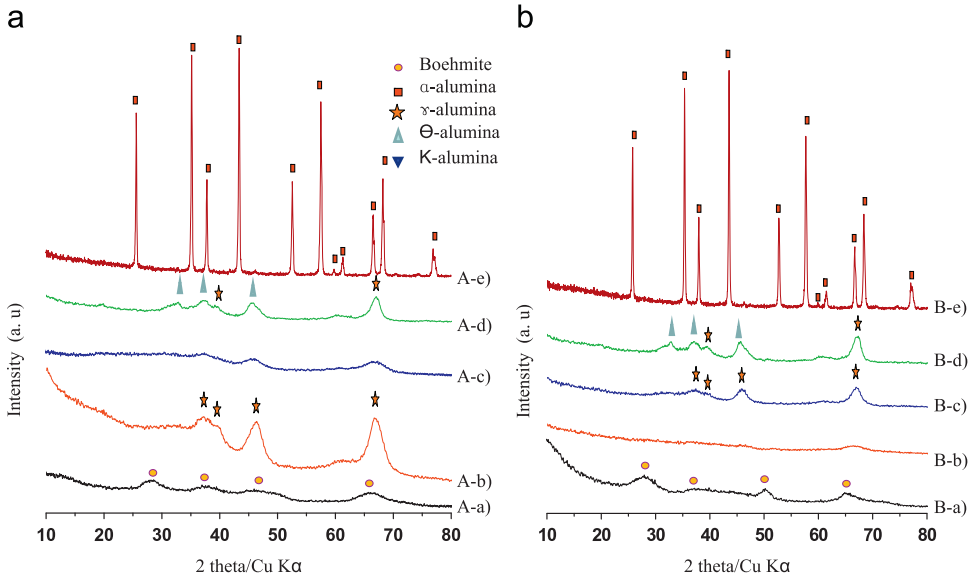

Fig. 2. The XRD patterns of the Al_2O_3 phases prepared at various calcinations temperatures, and without (A) or with (B) ethylenediamine at pH = 9 with AIP precursor. (A-a), (A-b), (A-c), (A-d), and (A-e) samples thermally treated at 400, 600, 800, 1000, and 1200 °C, respectively; (B-a), (B-b), (B-c), (B-d), and (B-e) samples thermally treated at 200, 400, 600, 8000, and 1000 °C, respectively.

This figure revealed that the shapes varied according to the pH and Al precursor. To avoid complication, we name the generated materials as the following: the materials named α-a, α-b, and α-c were prepared with AIP precursor at pH = 3, 7, and 9, respectively, and α-d material was prepared with AIP precursor and ethylenediamine at pH = 9. α-e and α-f materials were prepared with $Al(OH)_3$ precursor at pH = 3 and 7, and α-g material was prepared with AlO(OH) precursor at pH = 7. These materials were thermally treated at 1200 °C except α-d which was treated at 1000 °C. In α-a, α-b, and α-c, the particles' size was larger in the high pH range than that in the low pH range. The interaction of a spherical crystal transforms the particle shape to a long rod form. This result corresponded well with the XRD result shown in Fig. 1. The TEM images shown below the figure suggested the presence of α-d crystal growth. After addition of ethylenediamine to AIP precursor in the experimental procedure, a ligand substitution reaction occurred between the isopropyl group in the aluminum precursor and ethylenediamine, resulting in the formation of a stable chelating complex at 200 °C. Slightly dense crystals sized 20–50 nm was produced by the heat treatment at an intermediate temperature of 400 °C. At high-temperature treatment of 1200 °C, the fully dense αAl_2O_3 was formed. On the other hand, when $Al(OH)_3$ was used as the precursor, even rhombohedral hexagonal-shaped particles were grown with a width of 3–5 μm, height of 1.0–1.5 μm, and length of 3–5 μm. In particular, the uniformity of shape at pH = 3 was greater than at pH = 7. Finally, the shape of α-g also showed a slightly twisted rhombohedral hexagonal type. These results demonstrated that the aluminum precursor exerts different effects on the specificity of AIP, and the shapes were similar to the cases of $Al(OH)_3$ and AlO(OH) precursors.

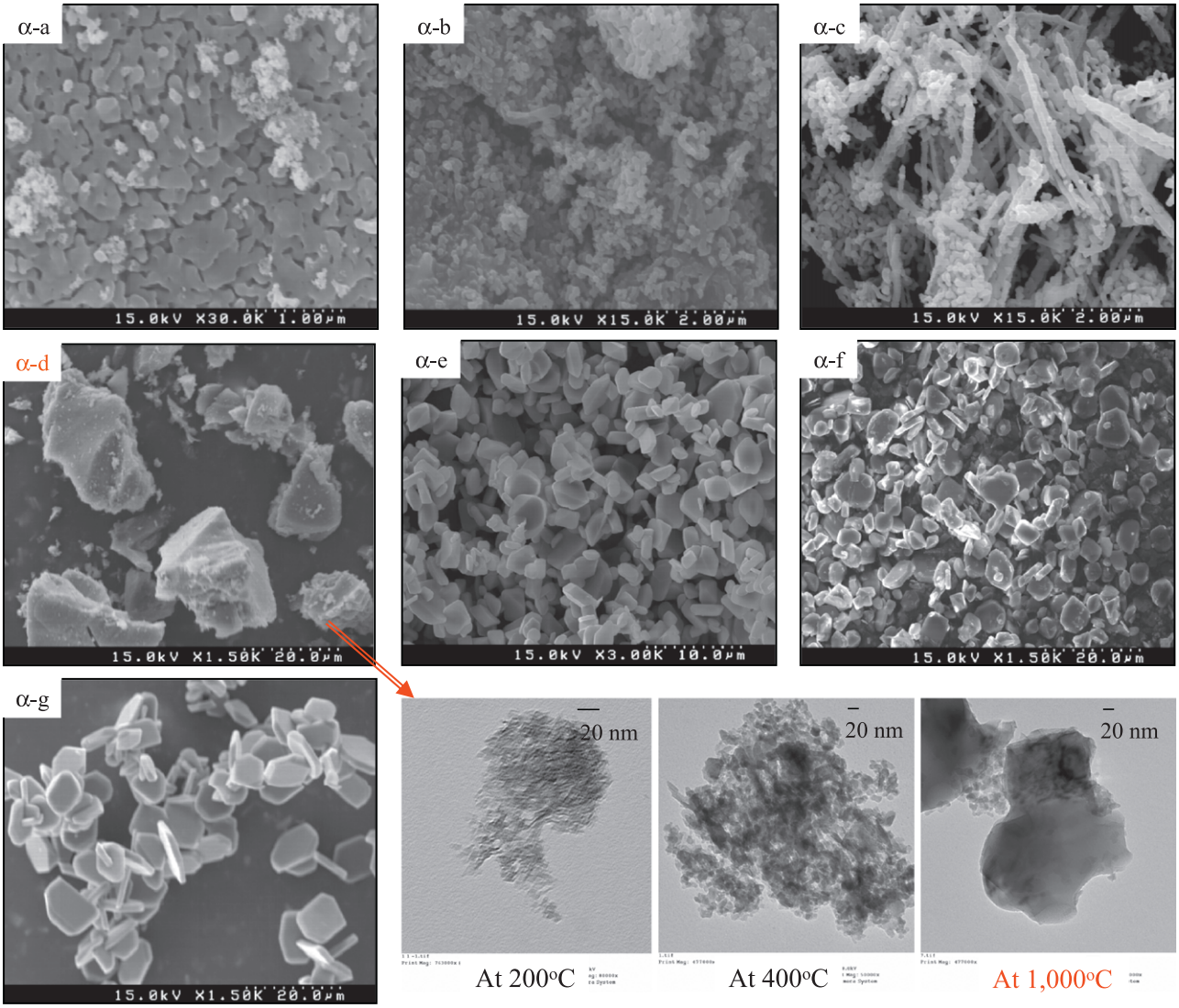

Fig. 3. The FESEM–TEM images of the α-Al_2O_3 particles prepared at various pHs and Al precursors. (α-a), (α-b), and (α-c) the α-Al_2O_3 powders were prepared with AIP precursor at pH = 3, 7, and 9, respectively; (α-d) α-Al_2O_3 was prepared with AIP precursor and ethylenediamine at pH = 9; (α-e) and (α-f) the α-Al_2O_3 powders were prepared with $Al(OH)_3$ precursor at pH = 3 and 7, respectively; (α-g) α-Al_2O_3 was prepared with AlO(OH) precursor at pH = 7.

The atomic compositions on the surface of the synthesized α-Al_2O_3 powders were analyzed by EDS and the results are summarized in Table 1, which revealed the presence of Al and O as the only elementary components of all the products with an Al:O atomic ratio of about 6:4. In the case of α-d, the molar ratio of Al to O obtained from EDS suggested slightly less O compared to the other samples. When a commercially available α-Al_2O_3 was tested by EDS measurement, the measured Al:O ratio of 68:32 revealed a much higher aluminum content than that of the synthesized samples, and a denser form. Our previous experience has demonstrated that a lower oxygen concentration and higher density result in a sapphire crystal with fewer defects, and a more regular and stable structure.

Adsorption–desorption isotherms of N_2 at 77 K for the α-Al_2O_3 powders were calculated and the values are summarized in Table 2. All the isotherms belonged to *I–V* types in the IUPAC classification [22]. They illustrate the shape and behavior of the N_2 adsorption isotherms for nanoparticle and porous materials. By using Kelvin's equation, the radius of the pore in which the capillary condensation occurs actively can be determined as a function of the relative pressure (P/P_0). The mean pore diameter, Dp, was calculated from $Dp=4VT/S$, where VT is the total volume of the pores, and S is the BET surface area. All of the α-Al_2O_3 powders in this study showed isotherms belong to III type in the IUPAC classification. The isotherm has been widely used, and a certain hysteresis slope can be observed at intermediate and high relative pressures in nano-materials, which are indicative of the presence of large nanopores. However, the synthesized α-Al_2O_3 samples in this study did not have any pores. Therefore, the pore volume was close to zero except α-b and α-d due to bulk pores. On the other hand, the BET surface area was more increased with the use of AIP precursor to 10–14 $m^2\,g^{-1}$, compared to zero with $Al(OH)_3$ and AlO(OH) precursors.

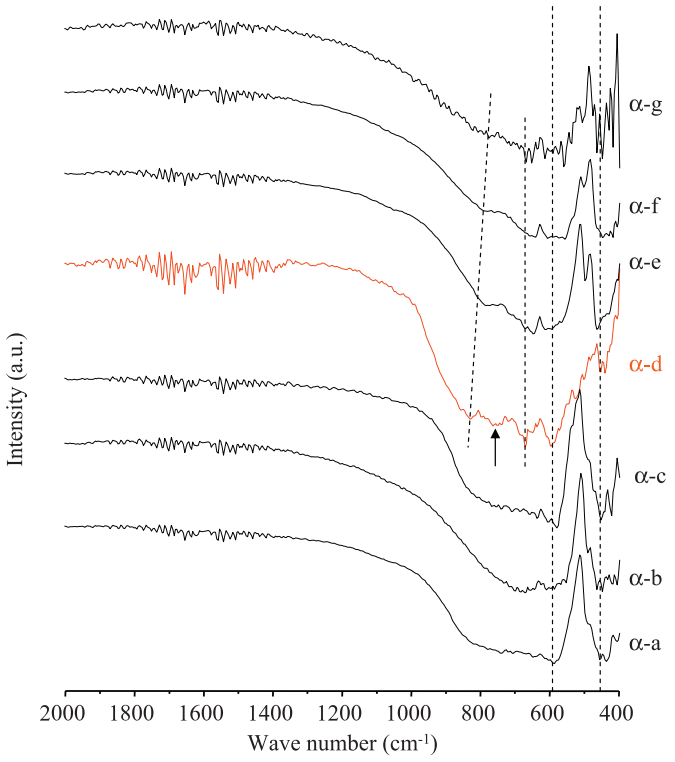

Fig. 4. FT-IR spectra of the synthesized α-Al_2O_3 materials. (α-a), (α-b), and (α-c) the α-Al_2O_3 powders were prepared with AIP precursor at pH=3, 7, and 9, respectively; (α-d) α-Al_2O_3 was prepared with AIP precursor and ethylenediamine at pH=9; (α-e) and (α-f) the α-Al_2O_3 powders were prepared with $Al(OH)_3$ precursor at pH=3 and 7, respectively; (α-g) α-Al_2O_3 was prepared with AlO(OH) precursor at pH=7.

Table 1
Atomic compositions on the surface of the synthesized α-Al_2O_3 powders were analyzed by energy-dispersive X-ray spectroscopy (EDS). α-a, α-b, and α-c: the α-Al_2O_3 powders were prepared with AIP precursor at pH=3, 7, and 9, respectively; α-d: α-Al_2O_3 was prepared with AIP precursor and ethylenediamine at pH=9; α-e and α-f: the α-Al_2O_3 powders were prepared with $Al(OH)_3$ precursor at pH=3 and 7, respectively; α-g: α-Al_2O_3 was prepared with AlO(OH) precursor at pH=7.

Elements/samples	Atomic % on the surface of α-Al_2O_3						
	α-a	α-b	α-c	α-d	α-e	α-f	α-g
O	63.12	60.39	62.52	64.02	61.81	55.57	59.12
A	36.88	39.61	37.48	35.98	38.19	44.43	40.88

Table 2
The BET surface areas calculated by adsorption–desorption isotherms of N_2 at 77 K for the α-Al_2O_3 powders. α-a, α-b, and α-c: the α-Al_2O_3 powders were prepared with AIP precursor at pH=3, 7, and 9, respectively; α-d: α-Al_2O_3 was prepared with AIP precursor and ethylenediamine at pH=9; α-e and α-f: the α-Al_2O_3 powders were prepared with $Al(OH)_3$ precursor at pH=3 and 7, respectively; α-g: α-Al_2O_3 was prepared with AlO(OH) precursor at pH=7.

Characters/samples	α-a	α-b	α-c	α-d	α-e	α-f	α-g
BET specific surface area (m^2/g)	13.79	9.99	12.38	10.25	0.87	0.81	0.73
Total pore volume (cm^3/g)	0.044	0.224	0.053	0.156	0.003	0.003	0.002
Average bulk pore diameter (nm)	12.70	89.80	17.08	60.91	11.51	11.91	10.66

Fig. 4 displays the FT-IR spectra of the synthesized α-Al_2O_3 powders. In general, the infrared spectrum of metal oxides can be classified into two vibration groups: internal vibrations of the framework TO_4, which are insensitive to structural vibration, and related to the external linkage of the TO_4 units in the structure. In all of the alumina samples in this study, there was no large band near 1078 cm^{-1} due to the asymmetric stretching of the internal AlO_4 tetrahedral. However, the two bands near 700 and 600 cm^{-1} were attributed to the symmetric stretching of the O–Al–O bond, with bends shown at around 450 cm^{-1}. At 450 cm^{-1}, the peak intensity was the strongest in the α-c and α-g samples which were synthesized with AIP and AlO(OH) precursors at pH=9 and 7, respectively; this result may be related to the crystal growth. The absence of any band-shift was attributed to the different tetrahedral environment produced by the structural distortion [23].

The zeta potential is an important parameter in colloidal stability, since it reflects the variation in surface potential for a specific material. These powders were derived from the solution route at low temperature; therefore, zeta potential studies were conducted to understand the surface charge of these powders. Table 3 shows the zeta-potential data of an aqueous suspension of synthesized α-Al_2O_3 at pH=7. No electrolyte was added to control the ionic strength of the solutions. The α-Al_2O_3 particles were positively charged by using AIP precursor to a maximum of 22.11 mV (prepared at pH=3). Above this pH, the positive charges of the α-Al_2O_3 particles were decreased with the same trend of mobility. Otherwise, the α-Al_2O_3 particles were negatively charged with the use of $Al(OH)_3$ and AlO(OH) precursors to a maximum of −23.25 mV (prepared with $Al(OH)_3$ precursor and pH=3). Importantly, the surface charge was highly negative with ethylenediamine additive despite the use of AIP precursor, resulting in the fastest mobility with an average aggregated diameter of 387 mm. The powder synthesized in the presence of ethylenediamine was assumed to have a higher negative charge on the surface even when using AIP precursor.

Fig. 5 presents the typical survey and high-resolution spectra obtained from the quantitative XPS analyses of the α-Al_2O_3 materials. The survey spectra of the particles contained Al_{2p} and O_{1s} peaks, as analyzed according to an XPS

Table 3
Zeta-potential data of an aqueous suspension of synthesized α-Al_2O_3 at pH=7. α-a, α-b, and α-c: the α-Al_2O_3 powders were prepared with AIP precursor at pH=3, 7, and 9, respectively; α-d: α-Al_2O_3 was prepared with AIP precursor and ethylenediamine at pH=9; α-e and α-f: the α-Al_2O_3 powders were prepared with $Al(OH)_3$ precursor at pH=3 and 7, respectively; α-g: α-Al_2O_3 was prepared with AlO(OH) precursor at pH=7.

Characters/samples	α-a	α-b	α-c	α-d	α-e	α-f	α-g
Zeta-potential (mV)	22.11	3.46	4.98	−29.38	−23.25	−19.56	−18.10
Mobility ($10^{-5}cm^2/Vs$)	4.438	0.6964	1.006	5.917	4.666	3.939	3.632
Average diameter (μm)	2.09	200.22	9.02	387.9	7.61	6.43	31.98

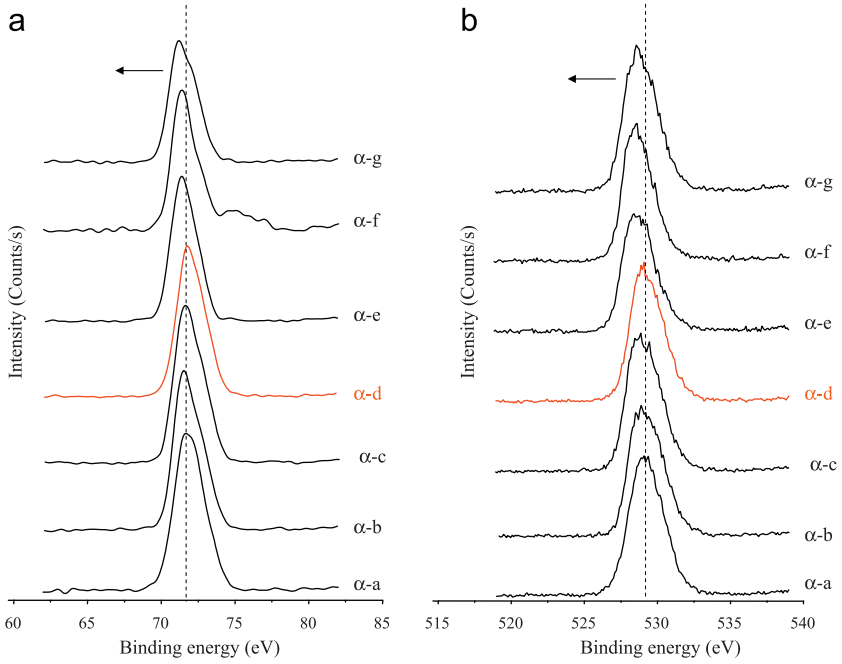

Fig. 5. The typical survey and high-resolution spectra obtained from the quantitative XPS analysis of the α-Al_2O_3 materials. (α-a), (α-b), and (α-c) the α-Al_2O_3 powders were prepared with AIP precursor at pH=3, 7, and 9, respectively; α-d α-Al_2O_3 was prepared with AIP precursor and ethylenediamine at pH=9; (α-e) and (α-f) the α-Al_2O_3 powders were prepared with $Al(OH)_3$ precursor at pH=3 and 7, respectively; (α-g) α-Al_2O_3 was prepared with AlO(OH) precursor at pH=7.

handbook [24]. It was well-known that the $Al_{2p3/2}$ orbital in alpha type Al_2O_3 is presented at 74.5 eV, which was assigned to Al^{3+} in Al_2O_3, but was surprisingly changed to a lower binding energy in all samples in this study, resulting in an $Al_{2p3/2}$ orbital at about 72.5 eV, which was assigned to reduced Al ions in Al_2O_3. Particularly, the $Al_{2p3/2}$ orbital in α-e–α-g with $Al(OH)_3$ and AlO(OH) precursors were shifted to a lower binding energy compared to those of α-a–α-d with AIP precursor. In general, a large binding energy indicates the presence of more oxidized states [24]. The O1s region was decomposed into two contributions: metal–O (−530.2 eV) in the metal oxide and metal–OH (531.0 eV∼). In general, a higher metal–OH peak indicated that the particles were more hydrophilic. However, only a single peak was seen in all the present samples at around 529 eV, which was assigned to Al–O. The O1s peaks were also distinguishably shifted in the samples α-e–α-g with $Al(OH)_3$ and AlO(OH) precursors, compared to those of α-a–α-d with AIP precursor.

4. Conclusions

In conclusion, α-Al_2O_3 rhombohedral structures were successfully fabricated, according to XRD and FT-IR results, after calcination at 1200 °C by using a sol–gel approach with AIP precursor at pH=3, 7, and 9, $Al(OH)_3$ precursor at pH=3, 7, and AlO(OH) precursor at pH=7. In particular, regulation via ethylenediamine as a chelating additive at a higher pH of 9 and AIP precursor allowed the use of a lower temperature of 1000 °C. In the BET analysis, all of the α-Al_2O_3 powders exhibited highly dense non-porous materials. The surface charges determined by ELS were affected by the Al precursor and ethylenediamine additive. The XPS result revealed that the Al species in the synthesized α-Al_2O_3 with ethylenediamine additive were close to reduced Al gradient rather perfectly Al^{3+}.

Acknowledgments

This research was financially supported by the Ministry of Education, Science Technology (MEST) and the National Research Foundation of Korea (NRF) through the Human Resource Training Project for Regional Innovation.

References

[1] H.-J. Kim, S. Odoul, C.-H. Lee, Y.-G. Kweon, The electrical insulation behavior and sealing effects of plasma-sprayed alumina-titania coatings, Surface and Coatings Technology 140 (2001) 293–301.
[2] T. Olding, M. Sayer, D. Barrow, Ceramic sol–gel composite coatings for electrical insulation, Thin Solid Films 398–399 (2001) 581–586.
[3] N.D. Kerness, T.Z. Hossain, S.C. Mcguirec, Impurity study of alumina and aluminum nitride ceramics: microelectronics packaging applications, Applied Radiation and Isotopes 48 (1997) 5–9.
[4] H. Lei, X. Wu, R. Chen, Preparation of porous alumina abrasives and their chemical mechanical polishing behavior, Thin Solid Films 520 (2012) 2868–2872.
[5] H. Lei, N. Bu, R. Chen, P. Hao, S. Neng, X. Tu, K. Yuen, Chemical mechanical polishing of hard disk substrate with α-alumina-g-polystyrene sulfonic acid composite abrasive, Thin Solid Films 518 (2010) 3792–3796.
[6] F. Cuccureddu, S. Murphy, I.V. Shvets, M. Porcu, H.W. Zandbergen, N.S. Sidorov, S.I. Bozhko, Surface morphology of c-plane sapphire (α-alumina) produced by high temperature anneal, Surface Science 604 (2010) 1294–1299.
[7] C.-H. Chen, J.-C. Chen, C.-W. Lu, C.-M. Liu, Numerical simulation of heat and fluid flows for sapphire single crystal growth by the Kyropoulos method, Journal of Crystal Growth 318 (2011) 162–167.
[8] N.R. de Tacconi, K. Rajeshwar, Semiconductor nanostructures in an alumina template matrix: micro versus macro-scale photoelectrochemical behavior, Electrochimica Acta 47 (2002) 2603–2613.
[9] S. Chokkaram, R. Srinivasan, D.R. Milburn, Burtron H. Davis, Conversion of 2-octanol over nickel-alumina, cobalt-alumina, and alumina catalysts, Journal of Molecular Catalysis A: Chemical 121 (1997) 157–169.
[10] J.A. Wang, X. Bokhimi, O. Novaro a, T. López, F. Tzompantzi, R. Gómez, J. Navarrete, M.E. Llanos, E. López-Salinas, Effects of structural defects and acid–basic properties on the activity and selectivity of isopropanol decomposition on nanocrystallite sol–gel alumina catalyst, Journal of Molecular Catalysis A: Chemical 137 (1999) 239–252.
[11] A. Boumaza, L. Favaro, J. Lédion, G. Sattonnay, J.B. Brubach, P. Berthet, A.M. Huntz, P. Roy, R. Tétot, Transition alumina phases induced by heat treatment of boehmite: an X-ray diffraction and infrared spectroscopy study, Journal of Solid State Chemistry 182 (2009) 1171–1176.
[12] A.C. Vieira Coelho, H. de Souza Santos, P.K. Kiyohara, K.N. Pinto Marcos, P. de Souza Santos, Crystal morphology and characterization of transition alumina powders from a new gibbsite precursor, Materials Research 10 (2007) 183–189.
[13] F. Mirjalili, M. Hasmaliza, L. Chuah Abdullah, Size-controlled synthesis of nano *a*-alumina particles through the sol–gel method, Ceramics International 36 (2010) 1253–1257.
[14] M.M. Martín-Ruiz, L.A. Pérez-Maqueda, T. Cordero, V. Balek, J. Subrt, N. Murafa, J. Pascual-Cosp, High surface area a-alumina preparation by using urban waste, Ceramics International 35 (2009) 2111–2117.
[15] S.-M. Kim, Y.-J. Lee, K.-W. Jun, J.-Y. Park, H.S. Potdar, Synthesis of thermo-stable high surface area alumina powder from sol–gel derived boehmite, Materials Chemistry and Physics 104 (2007) 56–61.
[16] J. Li, Y. Pan, C. Xiang, Q. Ge, J. Guo, Low temperature synthesis of ultrafine a-Al_2O_3 powder by a simple aqueous sol–gel process, Ceramics International 32 (2006) 587–591.
[17] M. Rajendran, A.K. Bhattacharya, Low-temperature formation of alpha alumina powders from carboxylate and mixed carboxylate precursors, Materials Letters 39 (1999) 188–195.
[18] H. Liu, G. Ning, Z. Gan, Y. Lin, A simple procedure to prepare spherical a-alumina powders, Materials Research Bulletin 44 (2009) 785–788.
[19] P. Souza Santos, H. Souza Santos, S.P. Toledo, Standard transition aluminas electron microscopy studies, Materials Research 3 (4) (2000) 104–114.
[20] H.-L. Wen, F.-S. Yen, Growth characteristics of boehmite-derived ultra"ne theta and alpha-alumina particles during phase transformation, Journal of Crystal Growth 208 (2000) 696–708.
[21] P. Mishra, Low-temperature synthesis of *a*-alumina from aluminum salt and urea, Materials Letters 55 (2002) 425–429.
[22] M. Khalfaoui, S. Knani, M.A. Hachicha, A. Ben Lamine, New theoretical expressions for the five adsorption type isotherms classified by BET based on statistical physics treatment, Journal of Colloid and Interface Science 263 (2003) 350–356.
[23] M. Di Vaira, A. Bianchi Orlandini, Crystal structure of a tetrahedrally distorted five-coordinated complex of Cobalt(I1) with the ligand Tris(2-diphenylphosphinoethy1)amine, Inorganic Chemistry 12 (6) (1973) 1–5.
[24] J.F. Moulder, W.F. Stickle, P.E. Sobal, K.D. Bomben, Handbook of X-ray Photoelectron Spectroscopy, Perkin-Elmer Corporation, 1992.